Characterization of Poly(vinylidene fluoride) Flat Sheet Membranes Prepared in Various Ratios of Water/Ethanol for Separator of Li-Ion Batteries: Morphology and Other Properties

Jun Young Han, Hyun-Hwan Oh, Kyung Jun Choi, Byoung Ryul Min

Department of Chemical and Biomolecular Engineering, Yonsei University, 262 Seongsanno, Seodaemun-gu, Seoul 120-749, South Korea

ABSTRACT: PVDF, poly(vinylidene fluoride), membranes were prepared and investigated by a scanning electron microscope, a universal testing machine, and capillary porometer for its potential use as a separator in lithium ion batteries. The membranes were prepared by phase inversion with different polymer types, concentrations of solution, amounts of additive, and nonsolvent ratios of water/ethanol. The morphology of membranes is affected by the ratio of both the coagulation bath (water/ethanol) and a low molecular weight additive (polymer/solvent/additive). The results showed that significant variations in the membrane were detected when adding an additive to the casting solution or ethanol to the coagulation bath. With an increased concentration of ethanol, the upper structure was found to be transformed into a sponge-like arrangement. In the case of Solef®1015 of the same polymer concentration, despite the higher molecular weight of 1015, a relatively small sized nucleus is formed, resulting in a denser network and relatively uniform membrane structure being formed. Mechanical testing showed that the tensile strength of the PVDF membranes increased when added to a 25 wt % ethanol coagulation bath, whereas it is decreased when added to higher concentrations of ethanol in the bath or additives in the casting solution. In a bath condition of water/ethanol = 75/25 wt % (Bath no. 2), the value of tensile strength is 7.11 and 7.52 MPa, for Solef®6010 20 wt % and Solef®1015 17 wt %, respectively. The thickness of the prepared membrane is 21–34 μm and the porosity is up to 50%. The electrolyte absorption changes of the fabricated membranes at different conditions are measured from 151 to 223 ± 15%. © 2011 Wiley Periodicals, Inc. J Appl Polym Sci 122: 2653–2665, 2011

Key words: membranes; morphology; mechanical properties; films; fluoropolymers; electrolyte absorption

INTRODUCTION

Recently, materials in the secondary battery have been a focus of interest. The separator plays a very important role in the battery. This membrane makes it possible for lithium ions to move through pore channels in a lithium ion battery and, at the same time, its insertion between the two electrodes prevents a short circuit that would be caused by any contact between the anode and cathode.[1,2] Separators are mainly manufactured from ion-exchange membranes, or microporous sheet membranes, in the form of a flat sheet prepared from polymeric materials. They must be electrically good insulators, and should have an aptitude for conducting ions by electrolyte or intrinsic ionic conduction. In particular, factors adversely influencing this transfer should be minimized for the best possible electrochemical energy efficiency of the batteries.[3–13]

Conventional battery cells are composed of positive/separator/negative/separator, thus two layers of separators are wound along with the electrodes. To ensure good contact at the interface they must be wound as tight as possible. Therefore, a strong separator is necessary to prevent any contact between electrodes. In addition, separator materials require a wide variety of properties including the following[6]: Electronic insulator, minimal electrolyte (ionic) resistance, mechanical and dimensional stability, sufficient physical strength to allow ease of handling, chemical resistance to degradation by electrolyte, impurities, and electrode reactants, effective in preventing migration of particles or colloidal or soluble species between the two electrodes, readily wetted by electrolyte, uniformity of thickness, and other properties. A typical battery cell uses a separator of 0.07–0.09 m², which is about 4–5% of total cell weight.[7]

Most microporous separators are produced by using a combination of polymeric materials. In general, they have micropores more than 0.01 μm. Microporous separators in low temperature applications of below 100°C, commonly use materials such as nonwoven fibers, polymer films [e.g., polyethylene (PE), polypropylene (PP)], and natural materials.

A PVdF-based polymer film can also be used as a separator and has attracted much attention because of their high ionic conductivity at room temperature and good thermodynamic stability advantages.[14,15] Currently, a microporous polymer film is produced by phase inversion technology because this process it a proven way obtain membranes of desired types and to adjust pores in the film.[16,17] By using the advantages of this method, prepared membranes can absorb a large amount of liquid electrolyte (with high porosity).[18] However, the application of fabricated films is limited due to a conflicting relationship between the tensile strength and the ionic conductivity. In other words, although ionic conductivity in the battery cell can be comparatively improved by increasing the pore diameter and porosity of the separator (polymer matrix), there is a tendency to reduce the tensile strength of the polymer film.[19] From this perspective, the research results of PVDF-based separators have been summarized in Table I, over the past 5 years.

In this work, PVDF-based membrane was prepared by phase inversion with various processes and conditions. It has the ability to be easily wetted by organic solvents, good compatibility with liquid electrolyte, and the ability to enable good electrode/electrolyte contact, when compared to polyolefin-based polyethylene.

PVDF-based Solef® 6010, 1015 which have different molecular weights, were used for researching the effect of its molecular weight on separators, and it was prepared with various concentrations to research the effect of polymer concentration on separators. 2-methoxyethanol, which is hydrophilic additive, was added to a polymer solution to study its effect on membrane morphology. The experiments were performed with various ratios of two nonsolvents (water/ethanol) in a coagulation bath and the resulting transformation was investigated. Also, the electrolyte absorption (wettability) of PVDF membrane was studied.

EXPERIMENTAL

Materials

Poly(vinylidene fluoride), of the commercial product name Solef® 6010(weight-average molecular weight, $M_W = 320,000$), and 1015(weight-average molecular weight, $M_W = 573,000$) was procured from the Sol-vay Korea, N-Methyl-2-Pyrrolidinone(NMP), and 2-Methoxyethanol were purchased from Kanto chemicals (Tokyo, Japan) and Samchun chemicals (Seoul, Korea), respectively. Ethylene Carbonate (EC), and Diethyl Carbonate (DEC) were purchased from Sigma Aldrich (Korea) and used without purification. Ethanol and Methanol were purchased from SK chemicals (Seongnam-si, Korea). All solvents and chemicals were reagent grade, and were used as received. The commercial separator of Celgard®2400 was procured from Welcos and has the specifications shown in Table II.

Preparation of porous separators

Casting solutions were prepared by dissolving PVDF in NMP at room temperature. Solef®6010 was dissolved by different molecular weight. Casting solutions of Solef®6010 17, 20 wt % and Solef®1015 8, 10, 12, and 17 wt % were prepared by stirring in 250 mL reactor. The similar viscous polymer solutions were prepared with different molecular weights. This is because viscosity is a very important factor for casting. Solef®1015 solution has a higher viscosity (almost 6 times) than Solef®6010 in a 17 wt % polymer concentration.

To evaluate the effect of additives in polymers, solutions were prepared by dissolving Solef®6010 and 2-methoxyethanol in NMP. The weight percent of Solef®6010 in NMP was fixed at 20 wt %. And the weight percent of 2-Methoxyethanol in casting solutions were prepared with 5, 10, and 15 wt %. In this instance, a condition of coagulation bath was prepared with water and ethanol, having a fixed weight ratio 75 : 25.

The homogeneous solutions were cast using a cast knife (Sheen, England) to 100 μm clearance casting-gap on the glass plates and then these were evaporated for 30 s. After the evaporation time, these were immersed in coagulation bath having various weight ratios of water/ethanol. As shown in Table III, Coagulation solvent, water/ethanol = x/y weight ratio to experiment with the conditions applied.

Membranes were kept in the methanol bath for a day, and dried in air. All these membranes were prepared at 40 ± 5% relative humidity and room temperature.

Characterization

Viscosity is a very importance factor in the process of casting. The viscosity of casting solutions was observed through a viscometer (DV-II + viscometer, BROOKFIELD). The Spindle number was LV-3 at 10 rpm.

The morphology of the surfaces and the cross section of the membranes were observed through a scanning electron microscope (JEOL JSM-5410LV),

TABLE I
A Brief Summary of Studies of PVDF Membrane for Separator in Recent 5 years[10,19–28]

Ref.	Year published	Polymer	Polymer manufacturer	Solvent	Additive	Method	Porosity (%)	Tensile strength (Mpa)	Electrolyte species (vol. ratio)	Electrolyte uptake (%)
19	2010	PVDF copolymer	Shanghai 3F	Acetone	MCM-41/SZ	Nonsolvent phase inversion	62.0	7.8	1M LiPF$_6$ in EC/DMC/DEC = 1:1:1	161.0
20	2009	PVDF-HFP	Aldrich	Acetone	PEGDMA	Dip coating and irradiaion	30–50	–	0.1M LiClO$_4$ in EC/DEC = 1:1	170–270
10	2009	PVDF	Solvay[a]	NMP	–	Nonsolvent phase inversion	58–77	4–5	1M LiPF$_6$ in EC/DMC = 1:1 (LP30®)	–
21	2009	PVDF	Kureha Chem	DMF	–	Electrospinning/Hot-press	45–50	17–58*	DEC	40–50
22	2009	PVDF	Kureha Chem	DMF	–	Electrospinning/press	69–76	Below 6.9	–	–
28	2008	PVDF-HFP	Elf Atochem[b]	DMF/Acetone	PEGDMA	Electrospinning/Heat-treated	70–76.6	3–6.5	DEC	267–352
23	2008	PVDF	Kureha Chem	DMF/Acetone	–	Electrospinning/Hot-press	60–70	Before 2.5, after 5–22	DEC	100–350
24	2008	PVDF	Atofina[c]	DMAc/Acetone	TiO$_2$	Electrospinning/Heat-treated	81–85	–	1M LiPF$_6$ in EC/DMC = 1:1	338–367
25	2007	PVDF-HFP	Elf Atochem	DMF/Acetone	PEG	Nonsolvent phase inversion	83–90.4	–	1M LiPF$_6$ in EC/DEC = 2:3	100–200
26	2007	PVDF-HFP	Aldrich	DMF	PVA	Preferential polymer dissolution	63–85.9	Nearly 9.5	1M LiClO$_4$ in EC/DEC = 1:1	65–90
27	2006	PVDF	Solvay[a]	DMF	–	Phase inversion/stretching	–	Before 11.5, after 52	1M LiPF$_6$ in EC/DEC/PC = 6:13:1	110–215

* Direction dependence.
[a] Solef®6020.
[b] Kynar®2801.
[c] Kynar®761.

TABLE II
Technical Data (Typical Properties) for Celgard® 2400

Basic Film Properties	Unit of Measure	Typical Value
Thickness	μm	25
Porosity	%	41
PP Pore Size (Avg. Diameter)	μm	0.043
Puncture Strength	Grams	450
Tensile Strength, MD	MPa	139.2
Tensile Strength, TD	MPa	13.7

after gold coating, to reduce the charge. The fractured cross sections of the membranes were achieved by breaking the samples with deep cooled in liquid nitrogen.

The mechanical properties of the membranes were observed using a universal testing machine (Mecmesin Coporation Mutitest 1-i). The maximum load cell was set at $50N$ and the crosshead speed was set at 50 mm/min, for all samples in the ambient environment. Load and extension measurements were automatically collected by a computer, which were used to calculate true strain and stress values for each sample, by considering the depth and width of the samples by extension.

The mean flow pore diameter and the pore distribution of prepared membranes were observed through an Auto capillary porometer (CFP-1200-AEL, PMI). The membranes were cut down to a suitable size and then immersed in POREWICK for 1 h. Measuring data was automatically collected by a computer.

The membranes were cut into a square in 25×25 mm^2. Each of them was accurately weighted in an electronic balance with a resolution of 0.001 g. The length and the width of the squared membranes were accurately measured by a micrometer with a resolution of 0.02 mm, and their thickness was ascertained by using a thickness-micrometer with a resolution of 0.001 mm. The apparent density (ρ) of the membranes was calculated from the obtained mass and the volume. Then, the porosity of the membranes was determined using the following the equation:

$$\text{Porosity } (\%) = (\rho_0 - \rho)/\rho_0 \times 100 \qquad (1)$$

TABLE III
Various Compositions of Coagulation Baths

No. of the Coagulation bath	Water (wt %)	Ethanol (wt %)
1	100	0
2	75	25
3	50	50
4	25	75
5	0	100

where, ρ_0 is the density of Solef®6010, 1015, that is, 1.78 g/cm^3. [9]

The electrolyte absorption of the membranes was determined by comparison of the mass difference of the membrane before and after incubation in EC(ethylene carbonate) and DEC (diethyl carbonate) 1 : 1 by volume, for 1 h. The mass (m) of the membrane after incubation was measured after removal from the liquid and blotting with a paper. On the basis of the following equation, the electrolyte absorption of the membrane was calculated[28]:

$$\text{Electrolyte absorption } (\%) = (m - m_0)/m_0 \times 100 \qquad (2)$$

where, m_0 is the mass of the membrane before the absorption process.

RESULTS AND DISCUSSION

Viscosity of polymer solution

Polymer viscosity is affected by its concentration and temperature and the viscosity of a casting solution affects the casting process. In the case of low viscosity, after casting, the casting thickness is thinner, due to the flow of solution. In the case of high viscosity, casting is difficult to achieve.

Solef®6010 of 17 and 20 wt % and Solef®1015 of 17 wt % solutions are prepared in NMP for measurement of viscosity. The viscosity of Solef®1015 17 wt % is 1183.6 cp (centipoises). The solution viscosity of Solef®6010 of 17, 20 wt %, are measured at 204.3 and 386.6 cp, respectively. As shown in Figure 1, Solef®1015 is up to 5.8 times higher in viscosity than Solef®6010 of 17 wt % and up to 3 times higher in viscosity than Solef®6010 of 20 wt %. It assumes that Solef®6010 of 20 wt %, and 386.6 cp, is appropriate for separators. Solef®1015 solution is prepared with different concentration 8, 10, and 12 wt % to
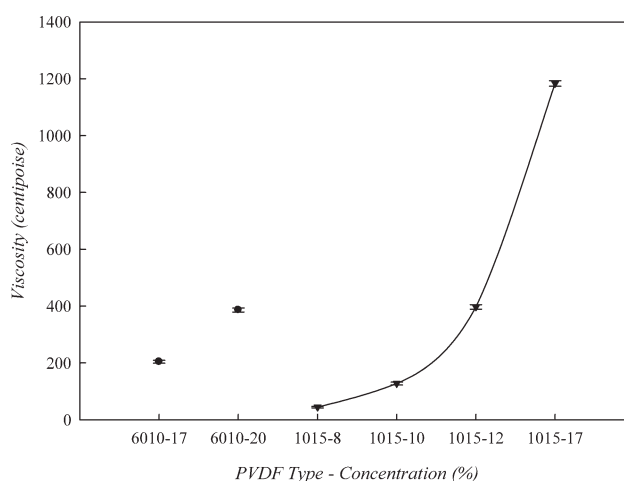

Figure 1 The viscosity of the casting solution with polymer type and concentration.
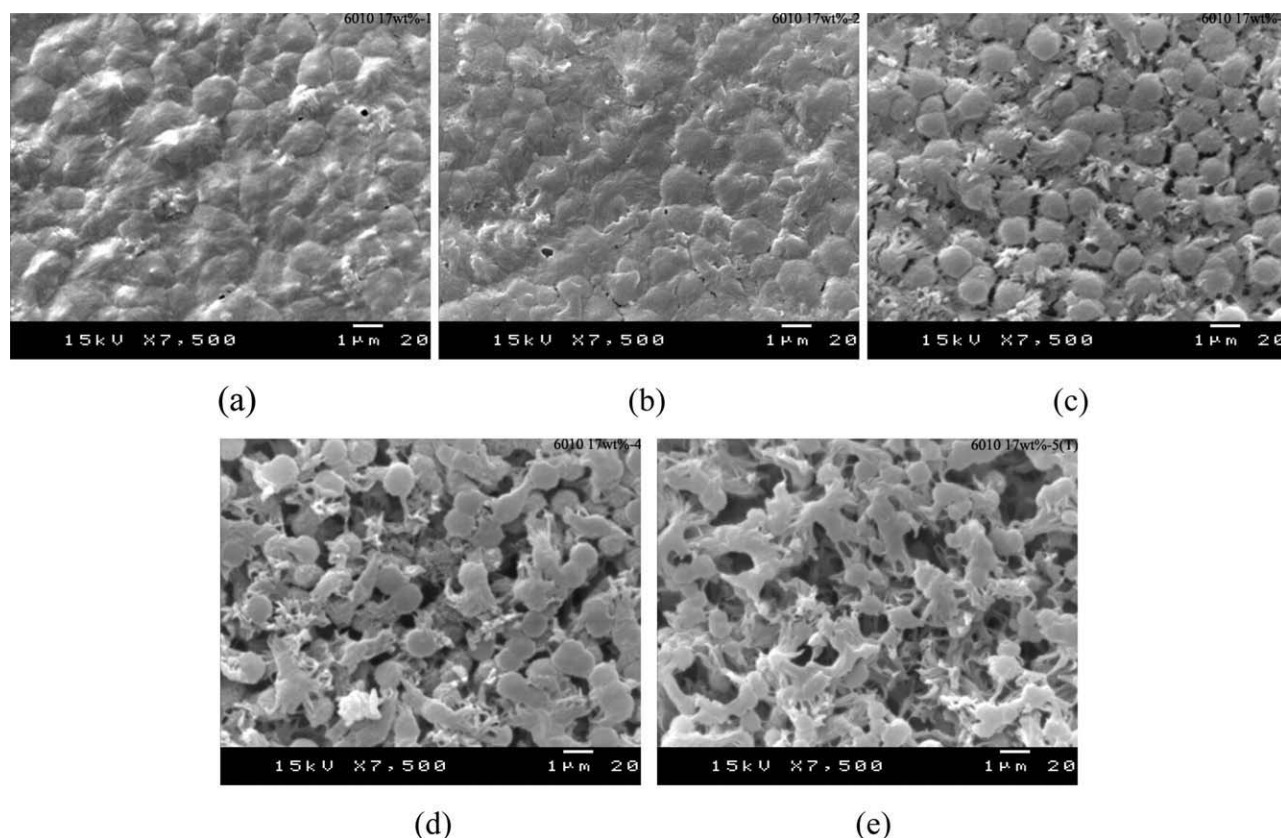
Figure 2 Top-surface images of membranes prepared from Solef®6010 17 wt % solution by coagulation into mixtures of water and ethanol. (a) Water, (b) Water : Ethanol = 75 : 25, (c) 50 : 50, (d) 25 : 75, and (e) ethanol.

search for appropriate viscosity similar to Solef®6010. After measurement, it is found that Solef®1015 of 12 wt % is 397.4 cp

Morphology of membranes

Topside surface structure of membranes with various coagulation baths

At fixed casting conditions, membranes prepared by the dry/wet phase inversion process, can be performed by polymer concentration and coagulation baths. In general, the dry/wet phase inversion process requires that the solution contains at least one volatile solvent for membrane formation. By the evaporation of some of this volatile solvent, the surface of the nascent casting solution will undergo a dry phase separation prior to its immersion in the coagulant.[29] However, in this work, the most common volatile solvents for polymer solutions, include NMP. And it is the purpose of porous membranes. Figures 2 and 3 represent a membrane surface, when coagulation baths were used in varying conditions, using Solef®6010, 1015 17 wt % dope solution. In the case of Solef®6010, using pure water did not form pores on the surface in semblance, but increasing the concentration of ethanol in the coagulation bath causes observable changes in the surface while

the network structure forms. It is considered that during the initial step the structure of the membrane surface formed by nucleation mechanism and then, in the formation stage, a growth mechanism occurred by entanglement of small nucleus formed by polymer chains. The network structure increases in nodular structure with increasing concentration of ethanol in the bath.

However, in the case of Solef®1015 of the same polymer concentration, despite the higher molecular weight of 1015, relatively small size of the nucleus is formed, the membrane structure formed was dense a network and relatively uniform. As a result, the more compact structure can be expected to have more strength.

Surface and cross section structure of Solef®6010 with various coagulation baths

The concentration of the dope solution was fixed at Solef®6010 20 wt % in NMP for preparation of the membrane. In Figures 4 and 5, surface and cross section are analyzed, respectively. The structure of surface is similar to the 17 wt %, however, the nodular size is smaller than the 17 wt %, in Figure 4.

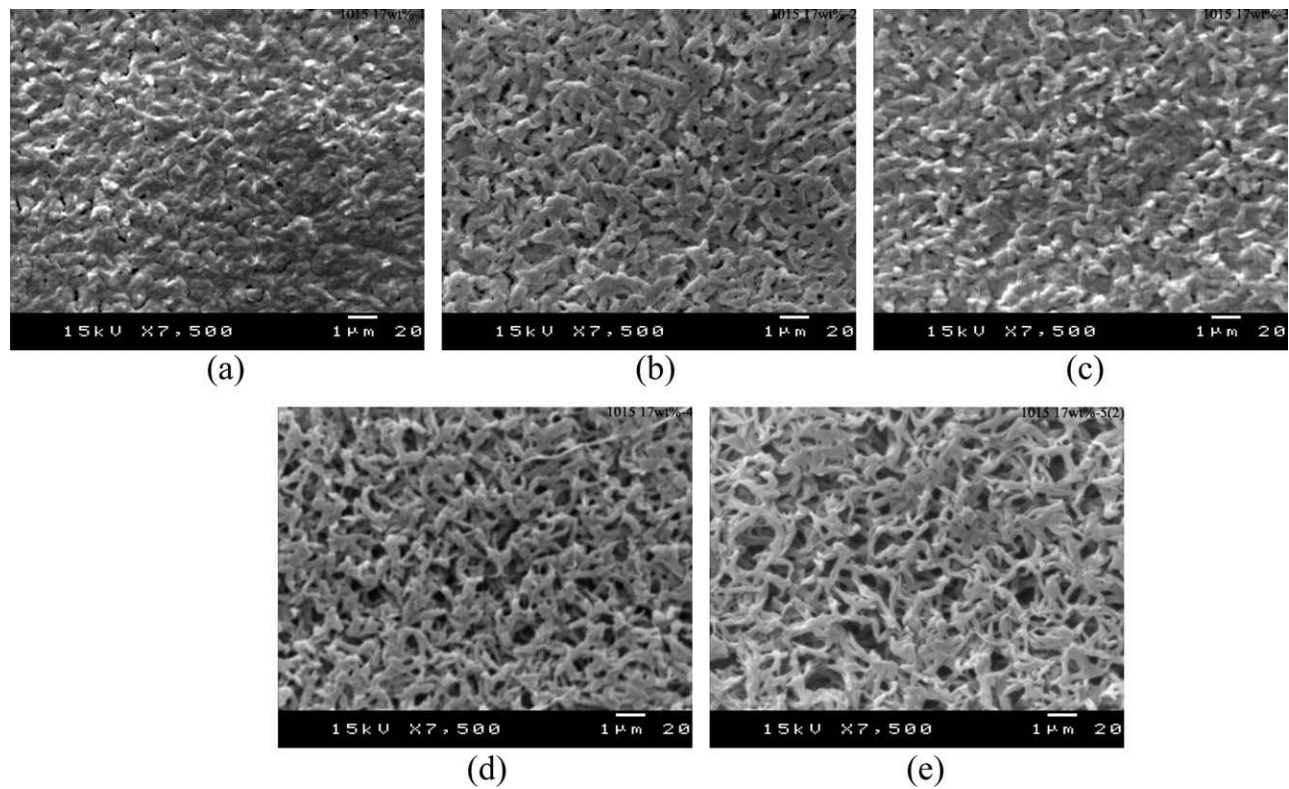Cross section structures of membranes are shown in Figure 5. Bath (a) membrane has small a sponge-

Figure 3 Top-surface images of membranes prepared from Solef®1015 17 wt % solution by coagulation into mixtures of water and ethanol. (a) Water, (b) Water : Ethanol = 75 : 25, (c) 50 : 50, (d) 25 : 75, and (e) ethanol.
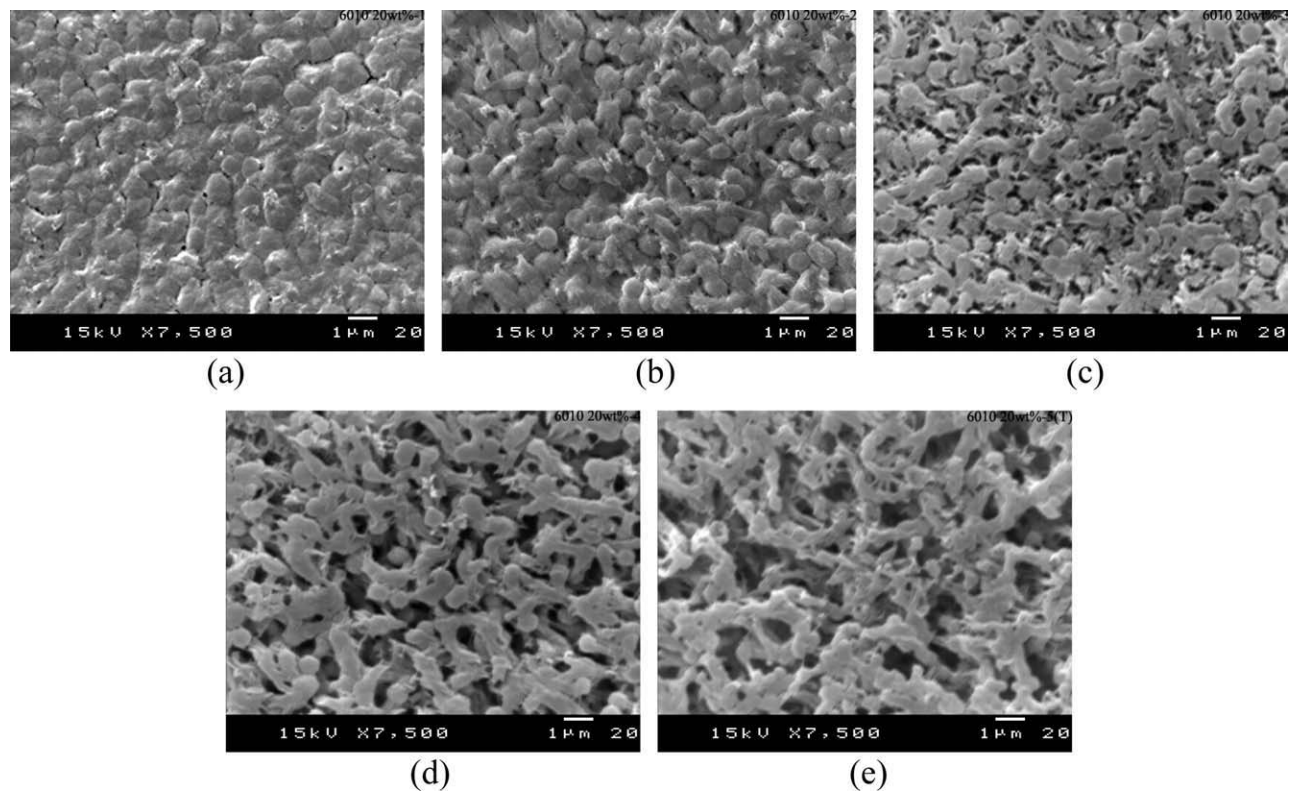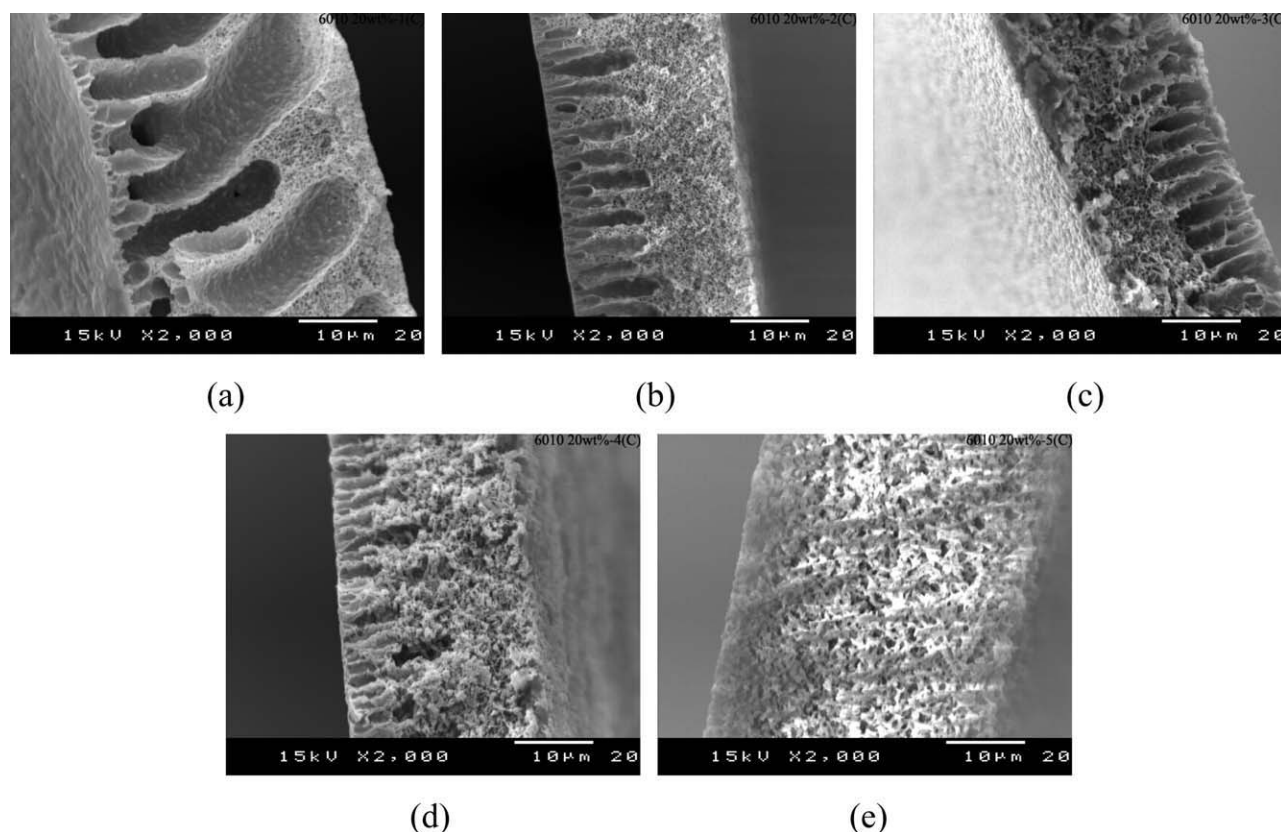

Figure 4 Top-surface images of membranes prepared from Solef®6010 20 wt % solution by coagulation into mixtures of water and ethanol. (a) Water, (b) Water : Ethanol = 75 : 25, (c) 50 : 50, (d) 25 : 75, and (e) ethanol.

Figure 5 Cross section images of membranes prepared from Solef®6010 20 wt % solution by coagulation into mixtures of water and ethanol. (a) Water, (b) Water : Ethanol = 75 : 25, (c) 50 : 50, (d) 25 : 75, and (e) ethanol.

like structure among large finger-like structures. In addition, it is represented that the finger-like structure is formed in top-layer with increasing concentrations of ethanol in the coagulation bath and sponge-like structure is formed in sublayer. With the increasing concentration of ethanol, it is found that the upper structure has been transformed into a sponge-like structure. It can be explained through critical solubility radius among the PVDF/NMP/Water/Ethanol. The critical solubility radius can be used to characterize the solvent/polymer interaction.[30] The critical solubility radiuses are 16.8 and 5.6 $(Jcm^{-3})^{1/2}$ for PVDF/water and PVDF/ethanol, respectively. The greater the critical solubility radius is the lower solubility. The solvent-nonsolvent mutual diffusivity has a big impact on cross section structure of membrane.[10,31]

After casting, membranes immerse in a coagulation bath and then nonsolvent penetrates the membrane to the inside. In case of nonsolvent water, a finger-like structure is formed because the water penetrates the cross section structure due to high diffusivity. Nonsolvent ethanol penetrates slowly into the casting solution due to low diffusivity. And diffusivity decreases with an increasing nonsolvent ethanol. In addition, while the nonsolvent penetrates to cross section and mixed solvent NMP, the diffu-

sivity is decreases, for this reason, Therefore, the membrane sublayer can be formed by the delay-demixing mechanism.[16] Consequently, the sponge-like structure is formed due to slow penetration rate of nonsolvent.

Figure 5 shows that a sponge-like structure clearly increases with increasing ethanol concentration. Even though membranes of Solef®6010 17 wt %, Solef®1015 15 wt % was not measured by SEM, it is considered that the membrane shows similar tendency.

In Figure 5(c,d), it is confirmed that finger-like structures of top layers in membrane have relatively obscure morphology and, as well, the sponge-like structure is not dense. This change of cross section structure in membrane affects mechanical strength (Noted on the mechanical properties).

Influence of a hydrophilic additive on membrane morphology

The influence of a hydrophilic additive on membrane morphology was investigated by using 2-metoxyethanol. The blend compositions were chosen at 5, 10, and 15 wt %. In this instance, a condition of coagulation bath was prepared by water and ethanol with a fixed weight ratio of 75 : 25. Figures 6 and 7
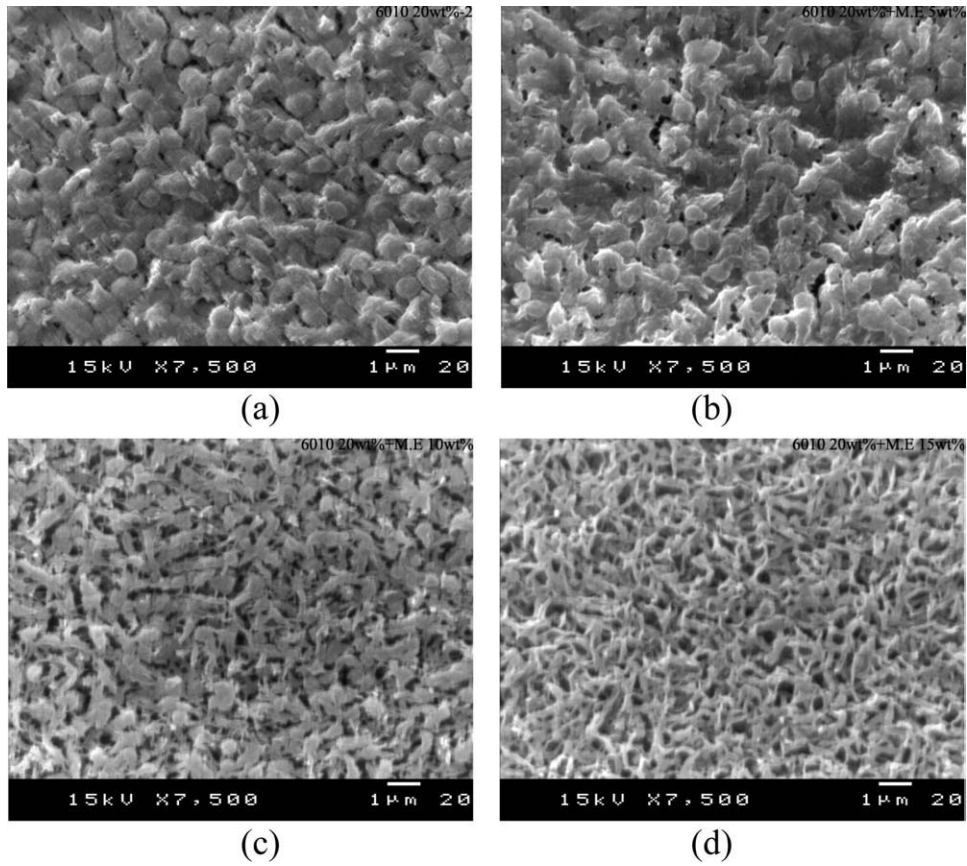
Figure 6 Top-surface images of membranes prepared from Solef®6010 20 wt % solution with adding different concentration 2-methoxyethanol. (a) 2-methoxyethanol 0%, (b) 5%, (c) 10%, and (d) 15%.
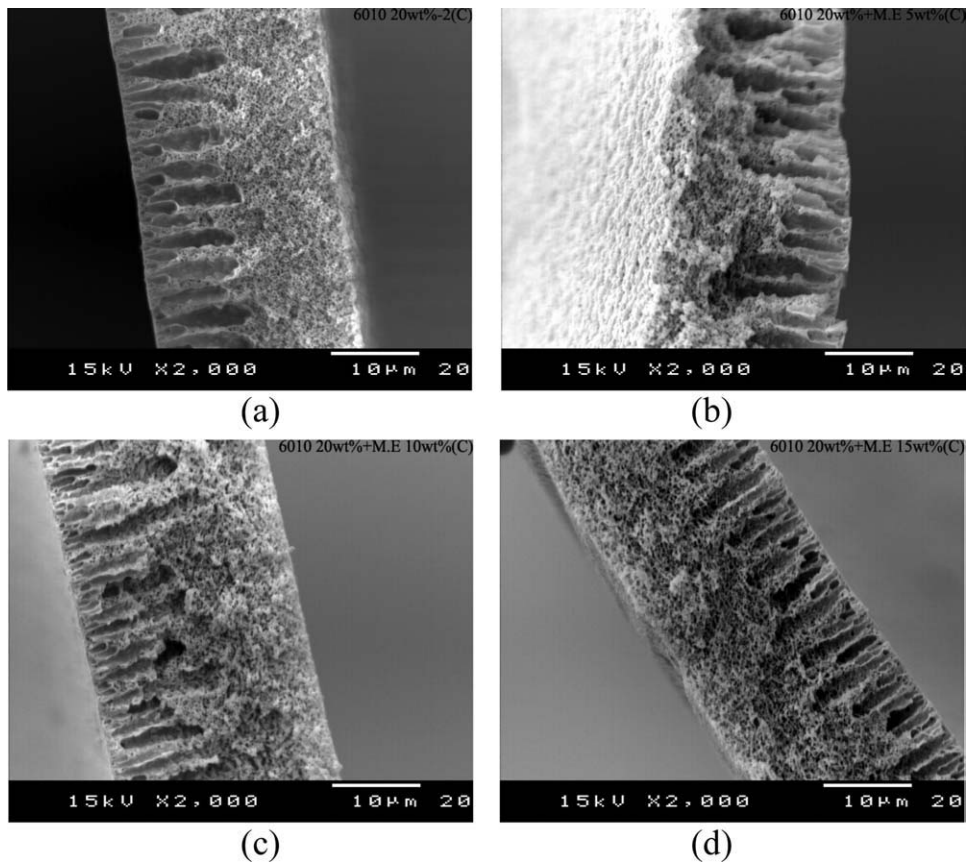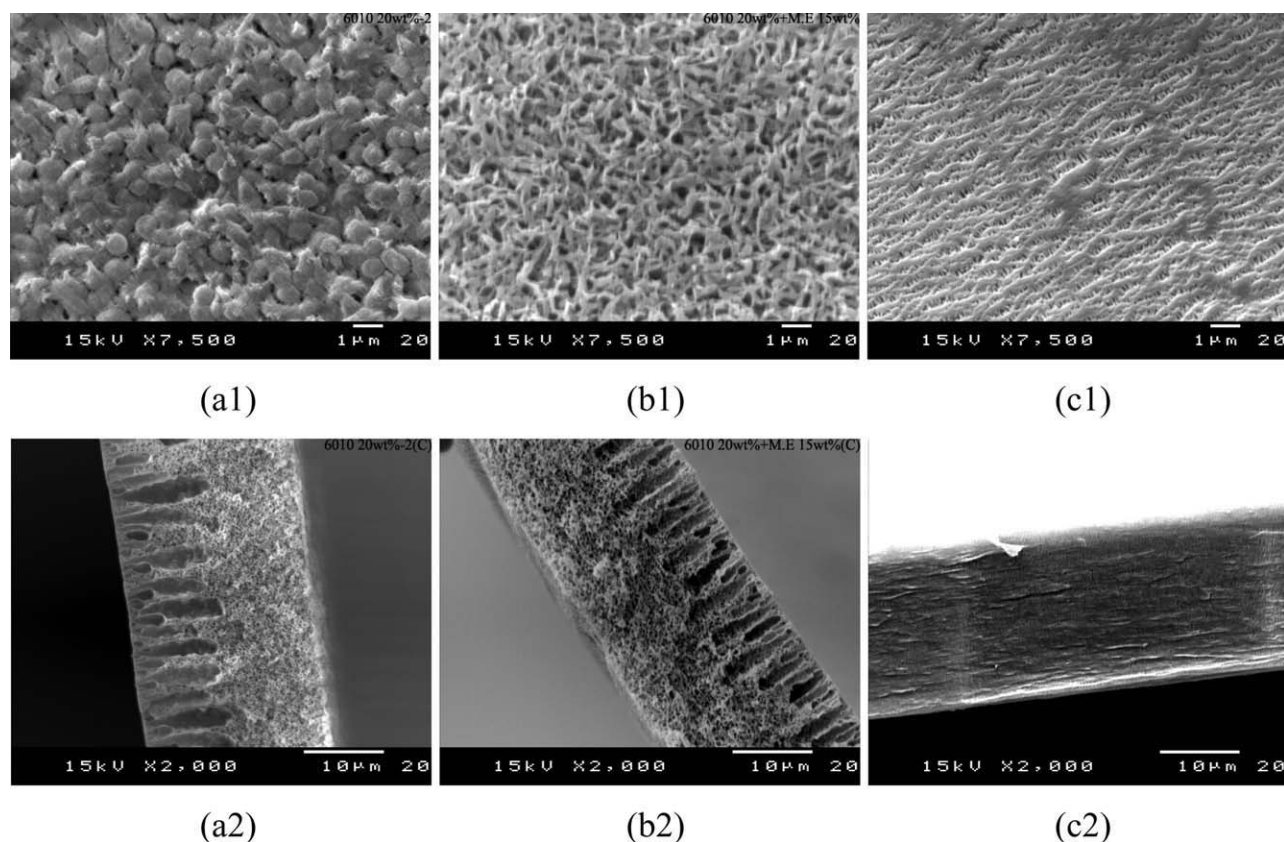

Figure 7 Cross section images of membranes prepared from Solef®6010 20 wt % solution with adding different concentration 2-methoxyethanol. (a) 2-methoxyethanol 0%, (b) 5%, (c) 10%, and (d) 15%.

Figure 8 Top-surface and cross section images of membranes prepared from Solef®6010 and Celgard®2400. (a) Solef®6010 20 wt % bath No. 2, (b) Solef®6010 20 wt % with additive 15 wt % bath No. 2, (c) Celgard®2400.

represent the effect of hydrophilic additive with Solef®6010 20 wt % on the membrane. As shown in Figure 6, the size of nodular formation is relatively small due to increasing concentrations of additives in the casting solutions and the surface structure is a homogeneous network. In addition, formed nuclei were reduced in size, becoming smaller with increased concentration of additives. It is suggested that, in the process of exchange of solvents and nonsolvent, the nonsolvent quickly penetrated the casting solution and liquid additives mixing rapidly with the nonsolvent. As shown Figures 5 and 7, in the case of using conosolvent of water/ethanol, the top-layer formed into the finger-like structures (macrovoide) and the sublayer formed a sponge-like structure. In the phase inversion process, Smolders et al.[32] empirically concluded that macrovoids formed in membrane prepared from ternary systems. In short, membranes without macrovoids are formed in the case of delayed demixing, except when the delay time is very short. However, macrovoids are formed in cases of instantaneous demixing, except when the polymer concentration and/or the nonsolvent concentration in the solution exceed a minimum value. However, the reason of the occurrence of macrovoids is complicated and exists as a multiplicity factor. Although we do not know the exact reciprocal diffusion (solvent and nonsolvent) of the top layer from the first moment in the film, as shown in Figures 5 and 7, we do know that the formation of macrovoids appeared membrane by instantaneous demixing mechanism.[16]

### Comparison of commercial separator and fabricated membrane Solef®6010

The top-side and cross section images of prepared Solef®6010 20 wt % in bath No. 2, with additive 15 wt % and Celgard®2400 are shown in Figure 8. It is clear from the images that the pores are uniformly distributed. However, the pore size of Solef®6010 membrane is substantially larger than Celgard®2400. The cross section image of Celgard®2400 has dense porous structure.

Thickness and porosity of membrane

Typically, the separators used have a thickness of base film 20–35 μm. Figure 9(a) shows the thickness of membranes differs respectively, with polymer concentration and types. However, the thickness is more affected by the coagulation bath. The thickness of membrane is reduced with increasing concentrations of ethanol in the coagulation bath. The
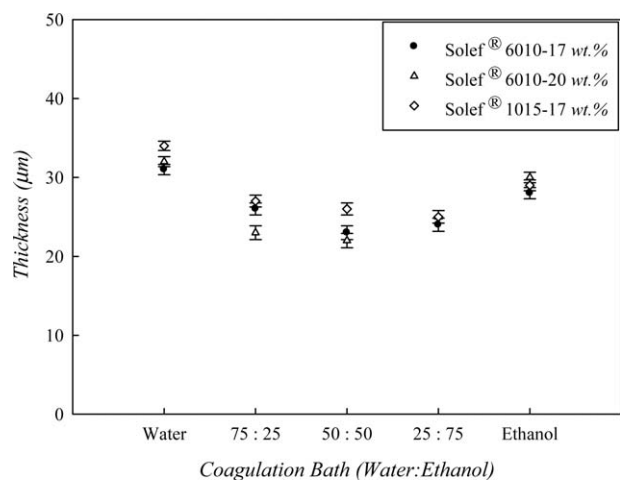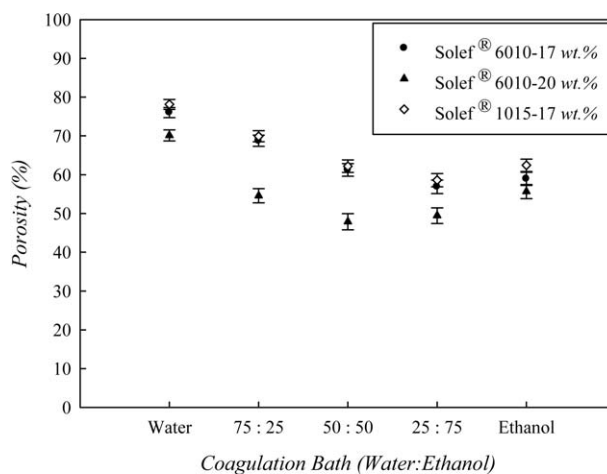
(a)
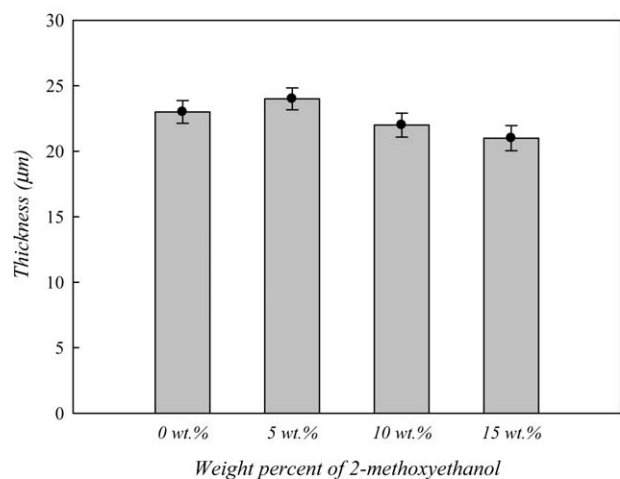
(b)

Figure 9 Thickness of membranes prepared from various conditions: (a) the effect of various coagulation bath conditions and (b) different weight percent of additive.

thickness of membrane in bath no. 5 (ethanol 100%), having fully sponge-like structures, slightly increases. In the case of using a pure water bath, the film thickness is thickest due to formed finger-like structures. This observation is determined with micrometer measurements and is corroborated by SEM, but with a slight difference in results. Thickness of commercial membrane requires under 30 μm. In this work, the thickness of prepared membrane is 21−34 μm. As shown in Figure 9(b), the thickness is slightly reduced with increasing concentrations of 2-methoxyethanol and porosity shows a decreasing tendency. Porosity decreases with increasing the concentration of ethanol in the coagulation bath and 2-methoxyethanol in a polymer solution as shown in Figure 10. It represents a macroscopic porosity decrease with increasing sponge-like structure. The porosity of prepared membranes range from 47.9 to 79.1% and is much higher than

with commercial membrane ranges between 30 and 40%. In contrast, the mechanical strength is very weak when compared with a membrane of a commercial separator because of using the nonsolvent induced phase inversion method.

Mechanical properties of membrane

In a general way, to increase the strength of a membrane, heat treatment is used. However, in this study, the tensile strength of the prepared membranes was measured without the post treatment. Figure 11(a) represents tensile strength of membranes with polymer types and concentrations. The membrane prepared from the coagulation bath conditioned water : ethanol = 75 : 25 wt % (Bath no. 2) was measured as the value of 7 MPa or more which has higher tensile strength than in other conditions. And the tensile strength is reduced due to increasing ethanol in the coagulation bath. In bath condition
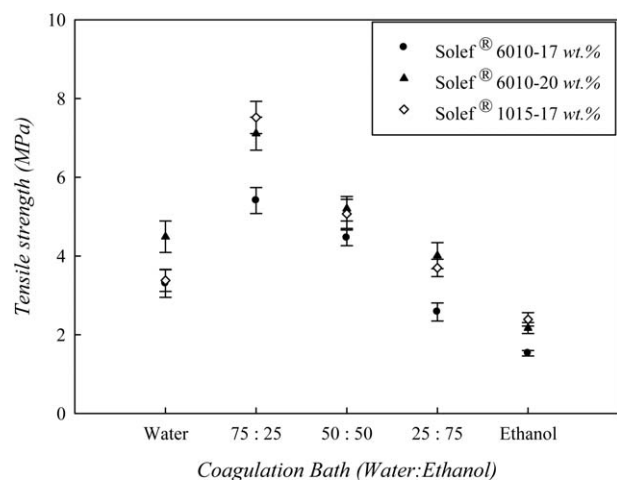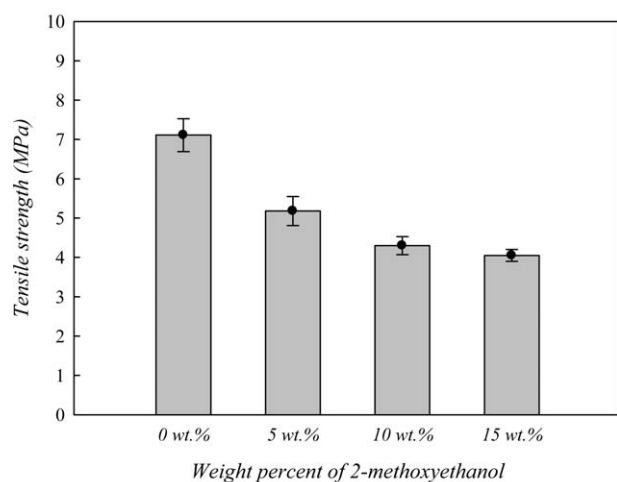

(a)
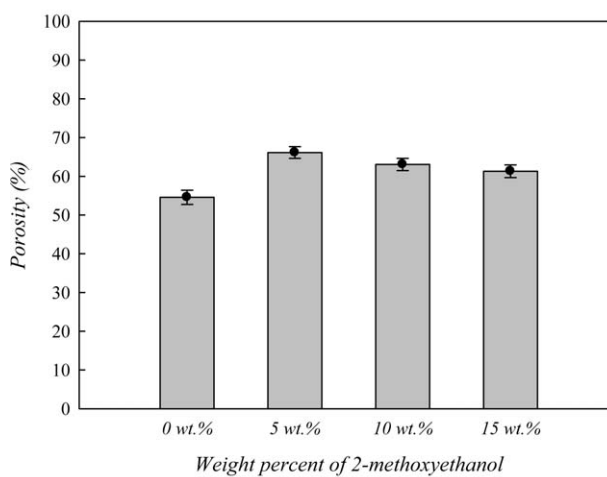
(b)

Figure 10 Porosity of membranes prepared from various conditions: (a) the effect of various coagulation bath conditions and (b) different weight percent of additive.
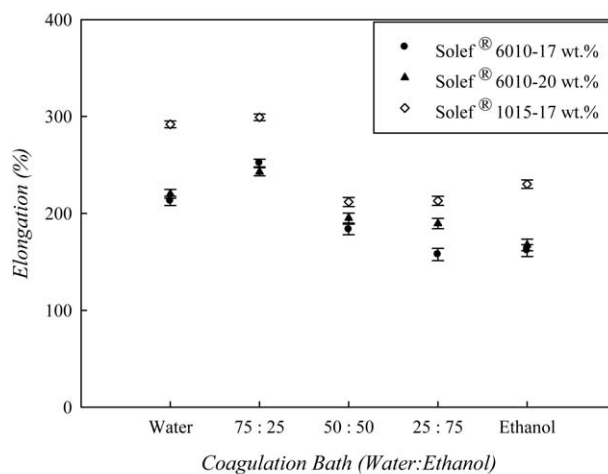
Figure 11 Tensile strength of membranes prepared from various conditions: (a) the effect of various coagulation bath conditions and (b) different weight percent of additive.

more than the molecular weight, or concentration, of polymer for control of the membrane. Mean pore size of Solef®6010 membrane in condition of no. 2 (water : ethanol = 75 : 25 wt %) coagulation bath is nearly 100 nm and maximum pore size distribution is higher than pure water bath. Mean pore size of bath no. 4 and 5 is from 225 to 722 nm. On the whole, the mean pore size increases with increasing concentrations of ethanol in the coagulation bath. In particular, in the case of Solef®1015 17 wt %, changes in pore size can be seen to be a relatively small reduction 139−276 nm, because the polymer has a larger molecular weight. A similar tendency is also observed with increasing concentrations of 2-methoxyethanol. However, membranes prepared in bath no. 3 could not be measured. It is supposed that these membranes cannot stand the pressure in instrument due to a defect of structure. It also occurred also in membrane case of 2-methoxyethanol 15 wt %.

no. 2, the value of tensile strength is 7.11 and 7.52 MPa for Solef®6010 20 wt % and Solef®1015 17 wt %, respectively. However, the value of bath no.1 (water 100%) is 4.49, 3.38 MPa. It can be inferred as follows. As seen in the morphology of cross section, it is convincing that because the membrane thickness is thinner, a relatively strong network in nodular structure has formed. Meanwhile, the addition of 2-methoxyethanol in polymer solution, as shown in Figure 11(b), the tensile strength is significantly decreased due to increasing concentrations of the additive, but elongation increased gradually, as indicated in Figure 12(b).
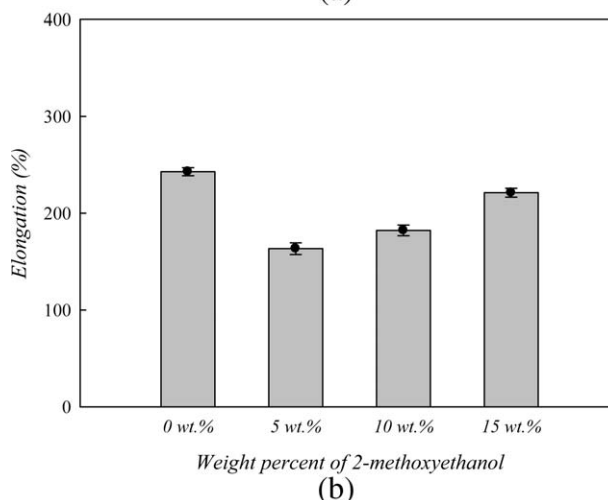
Pore size and pore distribution of membrane

As shown in Table IV, the pore size and distribution of the membrane were changed due to conditions of coagulation. The condition of coagulation is effective

Figure 12 Elongation of membranes prepared from various conditions: (a) the effect of various coagulation bath conditions and (b) different weight percent of additive.

TABLE 4
The Summary of Pore Size and Distribution of Membrane

Polymer	Concentration-Bath No.	Mean pore Diameter (nm)	Dia. At max pore Size distribution (nm)	Max. pore size Distribution (No.)
PVDF 1015	17-1	139	139	699,692
	17-2	125	125	152,532
	17-3		Not Detected	
	17-4	178	177	49,128
	17-5	276	275	21,879
PVDF 6010	17-1	121	121	42,304
	17-2	106	106	1,107,132
	17-3		Not Detected	
	17-4	369	367	7,961
	17-5	722	715	4,817
	20-1	111	113	16,297
	20-2	107	110	77,841
	20-3		Not Detected	
	20-4	225	225	354,065
	20-5	567	567	116,359
*Additive	20-M.E-5-2	133	133	95,825
	20-M.E-10-2	170	170	77,545
	20-M.E-15-2		Not Detected	

* Additive: 2-Methoxyethanol.

Discussions for applied separator

PVDF is widely used in the industrial production for fabricating ultrafiltration and microfiltration membranes because of excellent chemical resistance and thermal stability. It has also received much attention as primary material for the manufacture of separators in lithium ion batteries.[33] Recently, Poly(-vinylidene fluoride) and PVDF-HFP have been extensively investigated for applications to the rechargeable batteries.[34] The increase the pore size in the PVDF porous membrane contributed to enhance the ionic conductivity. As a result, it is possible to increase the cell rate capability. In addition, among the polymers, PVDF and PVDF-HFP have a high dielectric constant ($\varepsilon = 8.4$ F/m). By these characteristics, the PVDF matrix should conduces to greater ionization of the lithium salt to provide charge carriers. Particularly, due to a strong electron-withdrawing functional group (-C-F) in PVDF, polymer electrolytes are expected to be high stability in the positive potentials.[35,36]

PVDF membranes of high porosity can be fabricated by the phase inversion technique,[37] this process is a well-known method to get the membrane of a desired morphology through the controlled process.[38] By selecting the appropriate manufacturing process, PVDF membrane can be obtained as high electrical conductivity of 10^{-3} S/cm at room temperature, while maintaining good mechanical properties. And it has excellent wettability for a battery electrolyte. Through this way, it can be produced PVDF membranes, which can be absorb and retain large amounts of liquid electrolyte.[39,40]

In this study, the electrolyte absorption changes of the membranes at different conditions are measured from 151 to 223 ± 15%. The decreased porosity of the PVDF membranes could be the main reason for the drop of liquid absorption of the PVDF membranes.[23] Ultimately, the mechanical strength of the fabricated membranes is a lot weak than commercial separators. Therefore, using a support layer or the post heat treatment, the produced membrane could be a promising membrane for used as an electrolyte or separator in batteries.

CONCLUSIONS

A PVDF membrane was formed by nonsolvent induced phase inversion, and was investigated with concentration and molecular weight of PVDF, composition of coagulation bath and hydrophilic additive. The morphology of membranes is affected by the ratio of a coagulation bath and a low molecular weight additive. With an increasing concentration of ethanol, the upper structure was transformed into a sponge-like structure. In the case Solef®1015 of the same polymer concentration, despite the higher molecular weight of 1015, a relatively small size of nucleus is formed, resulting in a denser network and relatively uniform membrane structure being formed. Mechanical testing showed that the tensile strength of the PVDF membranes increased when added to the 25 wt % ethanol whereas it decreased when added to more ethanol in the bath or additive in the casting solution. A small amount of additive (in the casting solution and the coagulation bath) could effectively improve

the mechanical properties and morphology, whereas the porosity and electrolyte absorption of the PVDF membrane showed a small reduction.

References

1. Linden, D.; Reddy, T. B. Handbook of Batteries, 3rd ed.; McGraw-Hill: New York, 2002.
2. Besenhard, J. O., Ed. Handbook of Battery Materials; Wiley-VCH: Weinheim, Germany, 1999.
3. Hamano, K.; Yoshida, Y.; Shiota, H.; Shiraga, S.; Aihara, S.; Murai, M.; Inuzuka, T. U.S. Pat.6, 664,007, B2 (2003).
4. Sun, L.; Chen, G.; Xu, D.; Abe, T. Presented at the 204th Meeting of The Electrochemical Society, Orlando, Florida, 2003.
5. Sun, L. U.S. Pat.2003/0152828A1 (2003).
6. Pankaj, A.; Zhengming, J. Z. Chem Rev 2004, 104, 4419.
7. Johnson, B. A.; White, R. E. J Power Sources 1998, 70, 48.
8. Hoffman, H. G. Proceedings of the Tenth Annu Battery Conference on Applications and Adv, IEEE: New York, 1995; p 253.
9. Scheinbeim, J. I. Polymer Data Handbook, Oxford University Press: Oxford, 949 (1999).
10. Djian, D.; Alloin, F.; Martinet, S.; Lignier, H. J Power Sources 2009, 187, 575.
11. Linden, D.; Reddy, T. B. Handbook of Batteries, 3rd ed; McGraw-Hill: New York, 2002.
12. Besenhard, J. O., Ed.; Handbook of Battery Materials; Wiley-VCH: Weinheim, Germany, 1999.
13. Hamano, K.; Yoshida, Y.; Shiota, H.; Shiraga, S.; Aihara, S.; Murai, M.; Inuzuka, T. U.S. Pat.6,664,007, B2 (2003).
14. Periasamy, P.; Tatsumi, K.; Shikano, M.; Fujieda, T.; Saito, Y.; Sakai, T.; Mizuhata, M.; Kajinami, A.; Deki, S. J Power Sources 2000, 88, 269.
15. Saito, Y.; Capiglia, C.; Kataoka, H.; Yamamoto, H.; Ishikawa, H.; Mustarelli, P. Solid State Ionics 2000, 1161, 136.
16. Han, J.; Lee, W.; Chio, J. M.; Patel, R.; Min, B.-R. J Membr Sci 2010, 351, 141.
17. Magistris, A.; Quartarone, E.; Mustarelli, P.; Saito, Y.; Kataoka, H. Solid State Ionics 2002, 347, 152.
18. Michot, T.; Nishimoto, A.; Watanabe, M. Electrochim Acta 2000, 45, 1347.
19. Zhang, Y.; Zhang, G.; Du, T.; Zhang, L. Electrochimi Acta 2010, 55, 5793.
20. Sohn, J.-Y.; Im, J. S.; Gwon, S.-J.; Chio, J.-H.; Shin, J.; Nho, Y.-C. Radiat Phy Chem 2009, 78, 505.
21. Na, H.; Li, Q.; Sun, H.; Zhao, C.; Yuan, X. Polym Eng Sci 2009, 49, 1291.
22. Yang, C.; Jia, Z.; Guan, Z.; Wang, L. J Power Sources 2009, 198, 716.
23. Na, H.; Zhao, Y.; Zhao, C.; Zhao, C.; Yuan, X. Polym Eng Sci 2008, 48, 934.
24. Ding, Y.; Zhang, P.; Long, Z.; Jiang, Y.; Xu, F.; Di, W. Sci Technol Adv Mater 2008, 9, 015005.
25. Hwang, Y. J.; Jeong, S. K.; Nahm, K. S.; Manuel Stephan, A. Euro Polym J 2007, 43, 65.
26. Kalyana Sundaram, N. T.; Subramania, A. J Membr Sci 2007, 298, 1.
27. Seol, W.-H.; Lee, Y. M.; Park, J.-K. J Power Sources 2006, 163, 247.
28. Zhao, L.; Zhang, H.; Li, X.; Zhao, J.; Zhao, C.; Yuan, X. J App Polym Sci 2009, 111, 3104.
29. Pesek, S. C.; Koros, W. J. J Membr Sci 1993, 81, 71.
30. Hansen, C.; Beerbower, A. In: Kirk-Othmer Encyclopedia Chem Technology, 2nd ed.; Standen, A., Ed.; Wiley, New York, 1971; p 889.
31. Bottino, A.; Camera-Roda, G.; Capannelli, G.; Munari, S. J Membr Sci 1991, 57, 1.
32. Smolders, C. A.; Reuvers, A. J.; Boom, R. M.; Wienk, I. M. J Membr Sci 1992, 73, 259.
33. Strathaman, H.; Koch, K. Desalination 1977, 21, 241.
34. Sekhon, S. S.; Singh, H. P. Solid State Ionics 2002, 152/153, 169.
35. Michot, T.; Nishimoto, A.; Watanabe, M. Electrochim Acta 2002, 45, 1347.
36. Magistris, A.; Quartarone, E.; Mustarelli, P.; Saito, Y.; Kataoka, H. Solid State Ionics 2002, 152/153, 347.
37. Magistris, A.; Mustarelli, P.; Parazzoli, F.; Quatarone, E.; Piaggio, P.; Bottino, A. J Power Sources 2001, 97-98, 657.
38. Boudin, F.; Andrieu, X.; Jehoulet, C.; Olsen, I. I. J Power Sources 1999, 81/82, 804.
39. Song, J.; Wang, Y. Y.; Wun, C. C. J Power Sources 1999, 77, 183.
40. Choe, H. S.; Giacci, J.; Alamgir, M.; Abraham, K. M. Electrochim Acta 1995, 40, 228.